



Article

Targeted Disruption of *Lats1* and *Lats2* in Mice Impairs Testis Development and Alters Somatic Cell Fate

Nour Abou Nader, Amélie Ménard, Adrien Levasseur, Guillaume St-Jean , Derek Boerboom, Gustavo Zamberlam and Alexandre Boyer *

Centre de Recherche en Reproduction et Fertilité, Faculté de Médecine Vétérinaire, Université de Montréal, Saint-Hyacinthe, QC J2S 7C6, Canada

* Correspondence: alexandre.boyer.1@umontreal.ca; Tel.: +1-450-773-8521 (ext. 8345)

Abstract: Hippo signaling plays an essential role in the development of numerous tissues. Although it was previously shown that the transcriptional effectors of Hippo signaling Yes-associated protein (YAP) and transcriptional coactivator with PDZ-binding motif (TAZ) can fine-tune the regulation of sex differentiation genes in the testes, the role of Hippo signaling in testis development remains largely unknown. To further explore the role of Hippo signaling in the testes, we conditionally deleted the key Hippo kinases large tumor suppressor homolog kinases 1 and -2 (*Lats1* and *Lats2*, two kinases that antagonize YAP and TAZ transcriptional co-regulatory activity) in the somatic cells of the testes using an *Nr5a1*-cre strain (*Lats1*^{flox/flox};*Lats2*^{flox/flox};*Nr5a1*-cre). We report here that early stages of testis somatic cell differentiation were not affected in this model but progressive testis cord dysgenesis was observed starting at gestational day e14.5. Testis cord dysgenesis was further associated with the loss of polarity of the Sertoli cells and the loss of SOX9 expression but not WT1. In parallel with testis cord dysgenesis, a loss of steroidogenic gene expression associated with the appearance of myofibroblast-like cells in the interstitial space was also observed in mutant animals. Furthermore, the loss of YAP phosphorylation, the accumulation of nuclear TAZ (and YAP) in both the Sertoli and interstitial cell populations, and an increase in their transcriptional co-regulatory activity in the testes suggest that the observed phenotype could be attributed at least in part to YAP and TAZ. Taken together, our results suggest that Hippo signaling is required to maintain proper differentiation of testis somatic cells.

Keywords: Hippo signaling; *Lats1/2*; fetal Leydig cells; Sertoli cells; transgenic mouse model



Citation: Abou Nader, N.; Ménard, A.; Levasseur, A.; St-Jean, G.; Boerboom, D.; Zamberlam, G.; Boyer, A. Targeted Disruption of *Lats1* and *Lats2* in Mice Impairs Testis Development and Alters Somatic Cell Fate. *Int. J. Mol. Sci.* **2022**, *23*, 13585. <https://doi.org/10.3390/ijms232113585>

Academic Editor: Jacques J. Tremblay

Received: 3 October 2022

Accepted: 2 November 2022

Published: 5 November 2022

Publisher's Note: MDPI stays neutral with regard to jurisdictional claims in published maps and institutional affiliations.



Copyright: © 2022 by the authors. Licensee MDPI, Basel, Switzerland. This article is an open access article distributed under the terms and conditions of the Creative Commons Attribution (CC BY) license (<https://creativecommons.org/licenses/by/4.0/>).

1. Introduction

In mice, testes are first derived from the intermediate mesoderm and arise from the proliferation of coelomic epithelial cells. Thickening of the coelomic epithelia initially form the adrenogonadal primordium (AGP) at embryonic day 9.5 (e9.5), a structure from which the adrenal cortex also develops [1,2]. Following primordial germ cell migration (around e10.5), the AGP separates into two distinct tissues as the adrenal progenitor cells migrate dorsomedially at e11.0 [3]. Shortly after, the sex determining region of chromosome Y (SRY) is first expressed in a subpopulation of somatic cells of the gonadal primordium (GP) [4,5] which induces their differentiation into Sertoli cells via a positive feedback loop between SRY (sex-determining region Y)-box 9 (SOX9) and fibroblast growth factor 9 (FGF9) [6–8]. After Sertoli cell differentiation, another subpopulation of somatic cells differentiates into fetal Leydig cells (FLCs) following the secretion of desert hedgehog (DHH) by the differentiating Sertoli cells and subsequent activation of Hedgehog signaling [9–11]. Tracing experiments either alone or in combination with single-cell RNAseq suggest that both Sertoli cells and FLCs originate from a common progenitor cell population [12–14]. Numerous factors, including Wilm's tumor 1 (WT1) [15–18], nuclear receptor subfamily 5, group A, member 1 (NR5A1) [19], GATA binding protein 4 (GATA4) [20–22], insulin/insulin-like

growth factor [23,24], Sine-oculis-related homeobox-1 and 4 (SIX1/4) [25], or Chromobox2 (Cbx2) [26,27], are involved in early stages of testicular somatic cell differentiation but additional factors and pathways are likely involved.

Hippo is an evolutionarily conserved signaling pathway with well-established roles in cell fate determination and proliferation during embryonic development (reviewed in [28,29]). It consists of a kinase cascade that regulates two functionally redundant transcriptional co-activators, Yes-associated protein (YAP) and transcriptional coactivator with PDZ-binding motif (TAZ). In response to various extracellular signals, the mammalian STE20-like protein kinases 1 and -2 (MST1, MST2) are activated and phosphorylate the large tumor suppressor homolog kinases 1 and -2 (LATS1, LATS2), which in turn phosphorylate and inactivate YAP and TAZ [30–33]. When the cascade is inactivated, YAP and TAZ accumulate in the nucleus and interact principally with members of the TEA domain (TEAD) family of transcription factors to regulate the transcription of genes involved in cell growth, apoptosis, and proliferation [29,34].

Very little is known about the role of Hippo signaling in the testis, and most studies thus far have focused on its involvement in postnatal testicular physiology. Notably, it was shown that YAP is negatively regulated by FSH/PKA signaling in Sertoli cells [35,36] and that the number of YAP-positive Leydig cells increases in the mouse testis following chronic heat stress [37]. It was also shown that the loss of *Yap* and *Taz* decreases the expression of male sex-determining genes and increases the expression of female sex-determining genes in an immature Sertoli cell culture model [38], while the loss of *Lats1* and *Lats2* in granulosa cells have the opposite effect [39]. Finally, it was also demonstrated that the loss of Kindlin-2 (also known as fermitin family homolog 2; *Fermt2*) in Sertoli cells inhibits their proliferation and impairs cell–cell junction and blood–testis barrier maintenance by enhancing LATS1 interaction with YAP [40]. However, to this day, no studies have directly evaluated the role of LATS1 and LATS2, the core kinases of Hippo signaling, in testicular development.

In this study, we generated a mouse model in which *Lats1* and *Lats2* were conditionally deleted in testicular somatic cells to characterize the role of the Hippo signaling pathway in the development of the testes.

2. Results

2.1. Testicular Dysgenesis Is Observed following Concomitant Deletion of *Lats1* and *Lats2* in Testis Somatic Cells

To investigate the role of Hippo signaling in testicular development, we genetically disrupted the core Hippo pathway kinases *Lats1*, *Lats2*, or both in testicular somatic cells. To do this, mice bearing floxed alleles for *Lats1* and/or *Lats2* were crossed with a *Nr5a1-cre* [41] strain that drives the expression of Cre recombinase in the precursors of both Sertoli cells and FLCs of the developing testes. *Lats1*^{flox/flox};*Nr5a1-cre* and *Lats2*^{flox/flox};*Nr5a1-cre* mice developed normally, were healthy, had normal lifespans, and were fertile. Testes from *Lats1*^{flox/flox};*Nr5a1-cre* and *Lats2*^{flox/flox};*Nr5a1-cre* mice appeared normal at the gross and histologic levels and were therefore not further studied. Conversely, double cKO (*Lats1*^{flox/flox};*Lats2*^{flox/flox};*Nr5a1-cre*) mice died between 2 and 3 weeks of age of adrenal failure due to Cre expression in the adrenal cortex [42]. Gross morphological assessment showed that the testes from 2-week-old *Lats1*^{flox/flox};*Lats2*^{flox/flox};*Nr5a1-cre* mice were smaller than the testes from the control *Lats1*^{flox/flox};*Lats2*^{flox/flox} animals and had a distinctive, lobular appearance (Figure 1A).

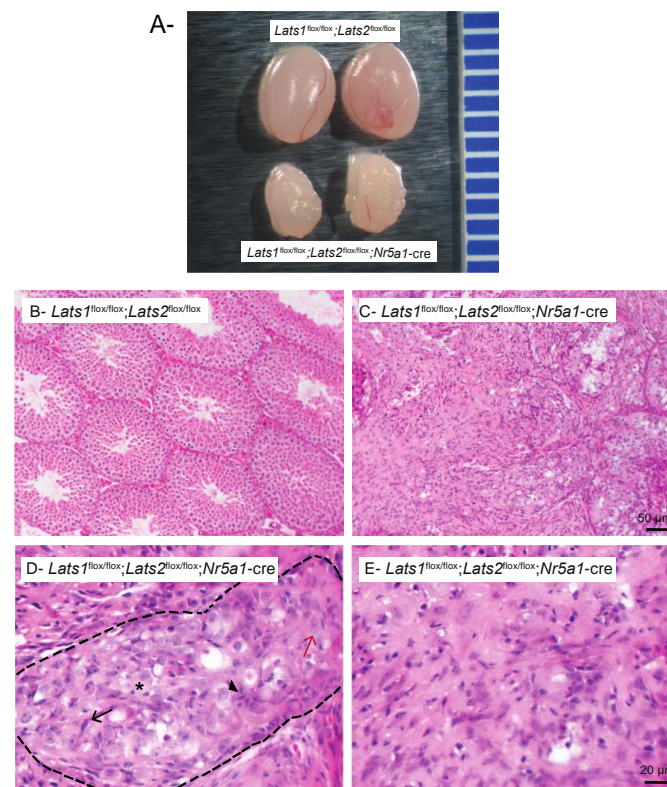


Figure 1. Testes of $Lats1^{flox/flox}; Lats2^{flox/flox}; Nr5a1-cre$ mice are larger than controls and are histomorphologically abnormal. (A) Photographs of testes from 2-week-old $Lats1^{flox/flox}; Lats2^{flox/flox}$ (control) and $Lats1^{flox/flox}; Lats2^{flox/flox}; Nr5a1-cre$ mice. Ruler graduations are in millimeters. (B,C) Photomicrographs comparing the testes of 2-week-old (B) $Lats1^{flox/flox}; Lats2^{flox/flox}$ and (C) $Lats1^{flox/flox}; Lats2^{flox/flox}; Nr5a1-cre$ mice. (D,E) Photomicrographs illustrating the remaining seminiferous tubules (D) and interstitium (E) in $Lats1^{flox/flox}; Lats2^{flox/flox}; Nr5a1-cre$ mice at higher magnification. Arrowhead = cells with a large nucleus and pale abundant cytoplasm. Red arrow = cell with an elongated large nucleus with an abundant cytoplasm. Black arrow = spindle-shaped cells. Asterisk = pyknotic cell. Dashes = delimitation of the seminiferous tubules. Scale bar in C is valid for B and scale bar in E is valid for D. Hematoxylin and eosin stain.

Histological analyses revealed striking abnormalities in the testes of $Lats1^{flox/flox}; Lats2^{flox/flox}; Nr5a1-cre$ mice. Seminiferous tubules were rarely observed and were very large, with disorganized cells and no lumen (Figure 1B–E). Several different types of cells were present within these tubules, with some cells having elongated large nuclei with an abundant cytoplasm, others having round large nuclei and abundant pale cytoplasm, others having a spindle shape, and others being pyknotic (Figure 1D). Furthermore, the tubules were surrounded by spindle-shaped interstitial cells reminiscent of fibroblasts or myofibroblasts (Figure 1E).

2.2. Testicular Dysgenesis Is First Observed at e14.5 in $Lats1^{flox/flox}; Lats2^{flox/flox}; Nr5a1-cre$ Mice

To analyze the onset and evolution of the phenotype observed in the testes of $Lats1^{flox/flox}; Lats2^{flox/flox}; Nr5a1-cre$ mice, embryos were collected from embryonic days e12.5 onward, and histopathologic examination of the developing testes was performed. These analyses showed that testes from e12.5 $Lats1^{flox/flox}; Lats2^{flox/flox}; Nr5a1-cre$ mice were phenotypically indistinguishable from age-matched controls (Figure 2) ($n = 6$). However, starting at e14.5, dysgenesis of a few testis cords became apparent in 30% of the mutant animals ($n = 10$) (Figure 2, dashed lines), while no abnormal phenotype was apparent in the remaining animals (Figure S1A). By e16.5, dysgenesis was apparent in a larger portion of the testis cords of all mutant animals ($n = 4$) and an accumulation of spindle-shaped

cells was apparent in some regions of the interstitium (Figure 2, red arrow). At e17.5, the phenotypic changes observed in the testes of *Lats1*^{flox/flox};*Lats2*^{flox/flox};*Nr5a1*-cre mice were exacerbated and dysgenesis was observed in all of the testis cords, with the Sertoli cells being disorganized and having a large prominent cytoplasm and the remaining germ cells being mostly apoptotic (Figure S2A, arrowhead) and pushed over to one side of the cords ($n = 10$) (Figure 2, arrow, Figure S2B). Testis cords were also larger than their control counterparts and the interstitium was mostly occupied by spindle-shaped cells (Figure 2). Phenotypic changes observed in the testes of *Lats1*^{flox/flox};*Lats2*^{flox/flox};*Nr5a1*-cre mice were even more pervasive and pronounced in testes of 1dpp mutant animals (Figure 2), with germ cells being absent in the majority of the tubules (Figure 2, Figure S2B), the presence of some spindle-shaped cells of indeterminate origin located inside the testis cords (Figure 2, arrowhead), and the interstitium being completely occupied by spindle-shaped cells.

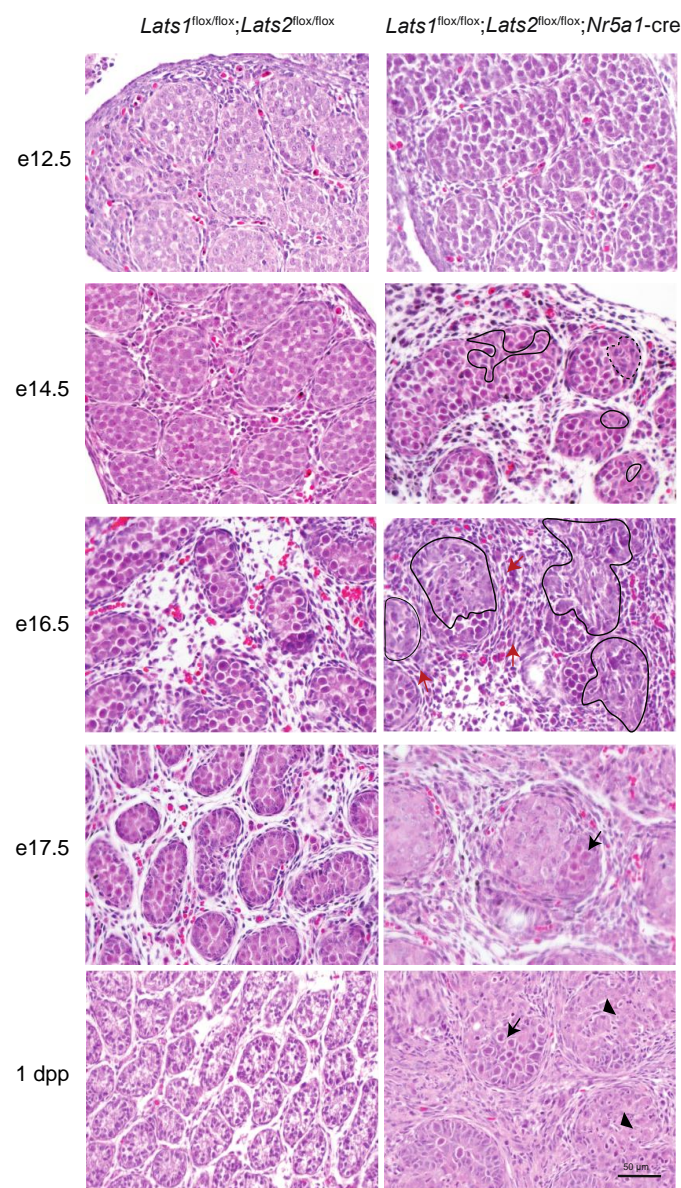


Figure 2. Progressive testicular dysgenesis in the *Lats1*^{flox/flox};*Lats2*^{flox/flox};*Nr5a1*-cre mice. Photomicrographs comparing testis histology of *Lats1*^{flox/flox};*Lats2*^{flox/flox};*Nr5a1*-cre with that of *Lats1*^{flox/flox};*Lats2*^{flox/flox} controls during development. Dashed lines = testis cords dysgenesis, black arrow = germ cells, red arrow = interstitial spindle-shaped cells, arrowhead = spindle-shaped cells in the testis cords. Scale bar (lower right) is valid for all images. Hematoxylin and eosin stain.

2.3. Hippo Signaling Is Inactivated in Late Stages of Testicular Differentiation

Although the *Nr5a1* promoter is active from the early stages of adrenal–gonadal primordium formation at around e9.0–e10 in mice [43], the phenotypic changes observed in the testes of *Lats1*^{flox/flox};*Lats2*^{flox/flox};*Nr5a1*-cre mice were not apparent until e14.5. This is later than expected but is consistent with the timing of phenotypic changes and inactivation of *Lats1* and *Lats2* observed in the developing adrenal glands of mutant animals, which is also first observed at e14.5 [42]. To determine if this was also the case in the testes, RT-qPCR analyses were performed on developing testes at embryonic days e14.5, e17.5 and 1dpp. The results showed a small but significant reduction (33%) of testis *Lats1* mRNA levels (but no reduction of *Last2* mRNA levels) in e14.5 mutant animals (Figure 3A); 56% and 42% decreases in testis *Lats1* and *Lats2* mRNA levels in e17.5 mutant animals (Figure 3B); and 60% and 58% decreases in testis *Lats1* and *Lats2* mRNA levels in 1dpp mutant animals (Figure 3C).

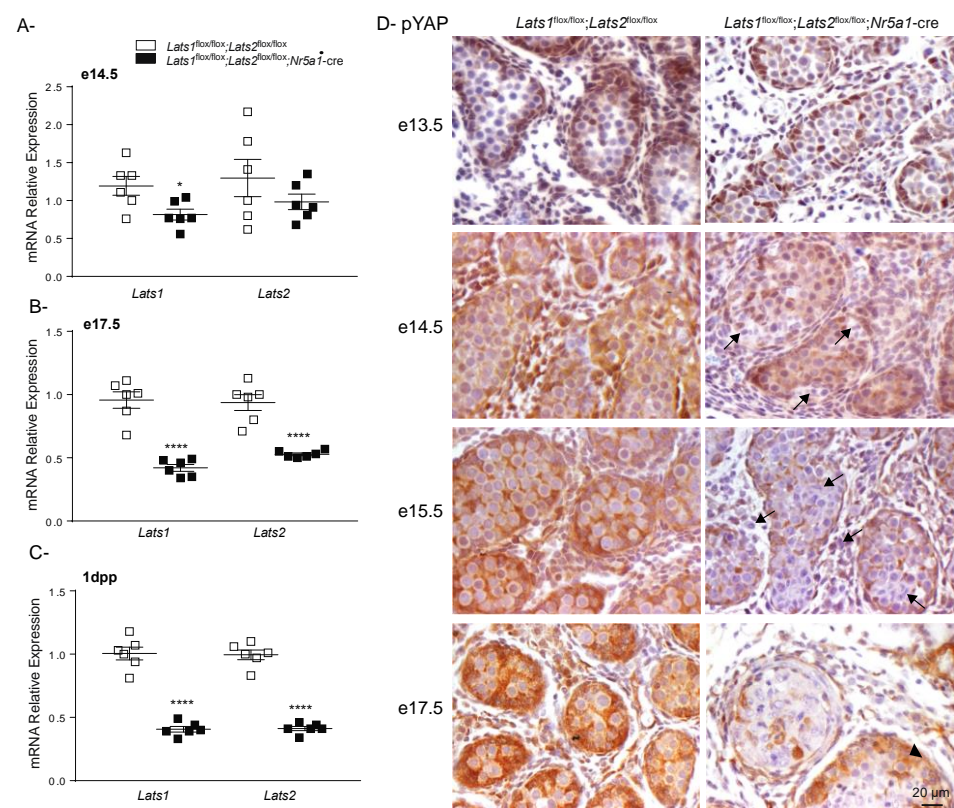


Figure 3. Efficiency of *Lats1* and *Lats2* knockdown in the testes of *Lats1*^{flox/flox};*Lats2*^{flox/flox};*Nr5a1*-cre mice. (A–C) RT-qPCR analysis of *Lats1* and *Lats2* mRNA levels in the testes of (A) e14.5, (B) e17.5, and (C) 1 dpp mice of the indicated genotypes ($n = 6$ animals/genotype). All data were normalized to the housekeeping gene *Rpl19* and are expressed as means (columns) \pm SEM (error bars). Asterisks = significantly different from control (* $p < 0.05$; **** $p < 0.0001$). (D) Immunohistochemical analysis of phospho-YAP expression in the testes of mice of the indicated genotypes. Scale bar (lower right) is valid for all images. Arrowhead = cells with inefficient recombination. Arrow = cells with efficient recombination.

We were unable to obtain quality immunohistochemistry for LATS1/2 to complement our RT-qPCR *Lats1/2* expression data. Loss of *Lats1* and *Lats2* was therefore assessed indirectly by evaluating the phosphorylation of their substrate YAP. At e13.5, phospho-YAP was readily detected in the nucleus of the Sertoli cells of both control and mutant testes (Figure 3D). Weak expression of phospho-YAP could also be detected in some interstitial cells of both control and mutant testes. These results suggest that Hippo signaling was not inactivated in mutant animals at this time point. At e14.5, phospho-YAP expression

was readily detected in the Sertoli cells and interstitial cells of the control testes (Figure 3D) and some mutant animals (Figure S1B). However, a decrease in the expression of phospho-YAP could be observed in a few Sertoli cells of some mutant animals (Figure 3D, Arrow). Furthermore, phospho-YAP expression remained weak and mostly cytoplasmic in the interstitium of these animals (Figure 3D). At e15.5 and e17.5, phospho-YAP expression remained elevated in both the interstitial cells and the Sertoli cells of control testes (Figure 3D). However, in the testes of the mutant animals, phospho-YAP was no longer detected in the majority of the interstitial cells (Figure 3D). Phospho-YAP expression was also lost in the majority (but not all) of the Sertoli cells, suggesting that recombination had not yet occurred in all Sertoli cells (Figure 3D, arrowhead). The pattern of expression of phospho-YAP is in accordance with the loss of *Lats1* and *Lats2* in the mutant animals and confirmed that inactivation of Hippo signaling occurs in both the FLCs and Sertoli cells. Variation between phospho-YAP expression in e14.5 mutant animals combined with the RT-qPCR data also suggests that recombination is initiated around that time point in mutant animals.

Since the inactivation of Hippo signaling is also normally associated with an increase in the nuclear localization of both YAP and TAZ, the expression of YAP and TAZ and their classic downstream targets were further evaluated at e17.5 by immunohistochemistry (using antibodies that mark both their phosphorylated and unphosphorylated forms). At this time point, YAP expression was detected in the cytoplasm and nucleus of most interstitial cells and in the Sertoli cells of control animals (Figure 4A,C). In the testes of mutant animals, expression of YAP was observed in the nucleus of most interstitial cells (Figure 4B,D). Nuclear, but generally weak, expression of YAP was detected in the Sertoli cells located in the middle of the tubules (Figure 4B,E) while strong YAP expression was observed in the Sertoli cells located at the periphery of some tubules (Figure 4B, arrow). However, this last population also expressed phospho-YAP (Figure 3D), suggesting that they correspond to Sertoli cells in which recombination did not occur. Weak TAZ expression was detected in the cytoplasm of the majority of Sertoli cells and some interstitial cells, as well as in the nucleus of rare interstitial cells in the control animals (Figure 4F,H). However, nuclear expression of TAZ was detected in a larger proportion of interstitial cells in the testes of *Lats1^{flox/flox};Lats2^{flox/flox};Nr5a1-cre* mice (Figure 4G,I). Furthermore, TAZ expression was detected in both the cytoplasm and nucleus of the recombined Sertoli cells (Figure 4G,J), suggesting that the increase of TAZ activity might play a greater role in the observed phenotype.

To further determine if the transcriptional co-regulatory activity of YAP and TAZ was increased in *Lats1^{flox/flox};Lats2^{flox/flox};Nr5a1-cre* mice, the mRNA levels of the well-established YAP/TAZ target genes ankyrin repeat domain 1 (*Ankrd1*), connective tissue growth factor (*Ctgf*), and cysteine-rich and angiogenic inducer 61 (*Cyr61*) were quantified by RT-qPCR. A 40-fold increase in the mRNA levels of *Ankrd1* and an 8-fold increase in the mRNA levels of *Ctgf* and *Cyr61* were observed in the testes of e17.5 *Lats1^{flox/flox};Lats2^{flox/flox};Nr5a1-cre* mice (Figure 4K), confirming that the expression of known targets of YAP and TAZ is increased in the testes of mutant animals. Taken together, these data suggest that transcriptional regulatory activity of YAP and/or TAZ is increased in the somatic cells of *Lats1^{flox/flox};Lats2^{flox/flox};Nr5a1-cre* mice, and most likely play a role in the observed phenotypic changes.

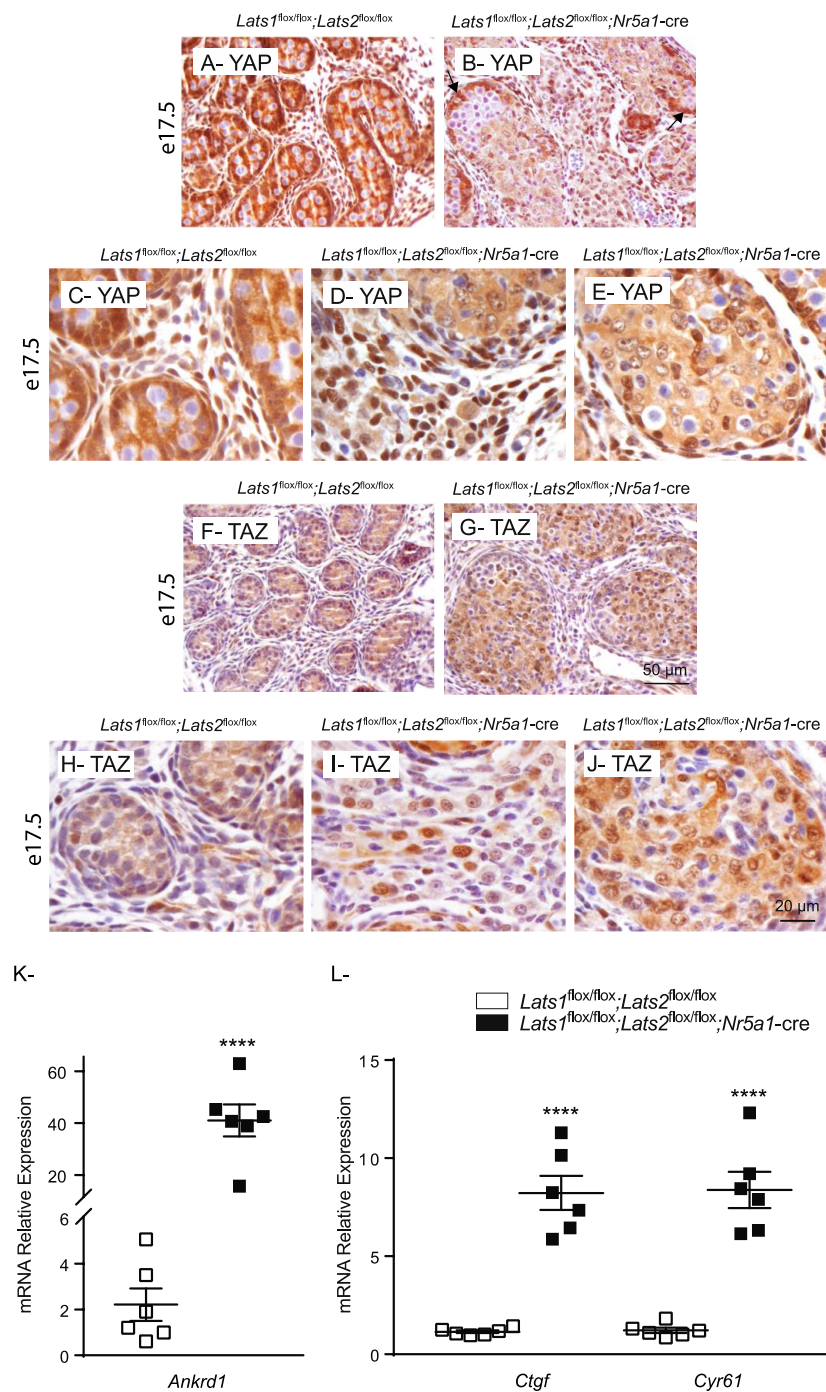


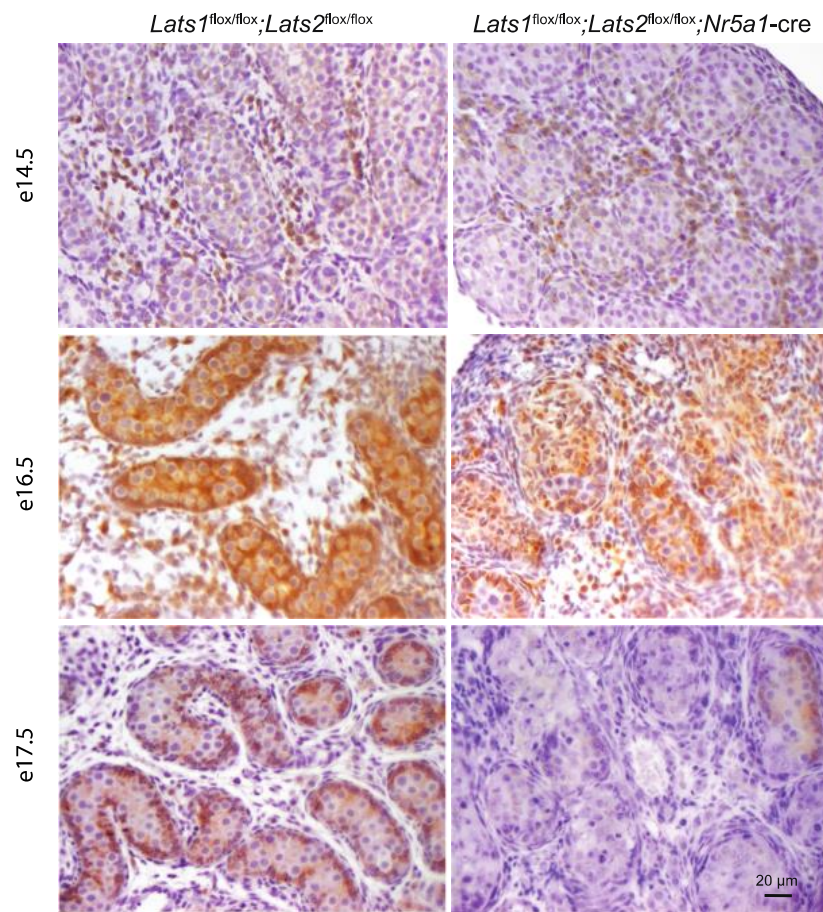
Figure 4. YAP/TAZ activity increases in the testes of *Lats1^{flox/flox};Lats2^{flox/flox};Nr5a1^{cre/+}* mice. (A–E) Immunohistochemical analysis of YAP expression in testes of e17.5 mice of the indicated genotypes. (F–J) Immunohistochemical analysis of TAZ expression in testes of e17.5 mice of the indicated genotypes. Arrow = YAP expression in non-recombined Sertoli cells. Scale bar in (G) is valid for (A,B,F). Scale bar in (J) is valid for (C–E,H,I). (K,L) RT-qPCR analysis of YAP/TAZ downstream targets mRNA levels in the testes of e17.5 mice of the indicated genotypes ($n = 6$ animals/genotype). All data were normalized to the housekeeping gene *Rpl19* and are expressed as means (columns) \pm SEM (error bars). Asterisks = significantly different from control (**** $p < 0.0001$).

2.4. Disruption of *Lats1* and *Lats2* Alters the Epithelization and the Differentiation of the Sertoli Cells during Testis Development

YAP and TAZ activation have been known to play key roles in processes such as epithelial-to-mesenchymal (EMT) transition and fibrosis, two cellular processes that share many molecular characteristics [44–46]. Misexpression of mesenchymal-associated pathways could explain both the loss polarity of Sertoli cells and the appearance of fibroblast/myofibroblast-like cells in the interstitial tissue. To determine if normal epithelization of the Sertoli cells was affected in the testes of mutant animals, markers of Sertoli cell junctions were then evaluated. Expression of GAP junction protein alpha-1 (GJA1), (an important component of Sertoli/Sertoli interactions [47,48]) expression was first analyzed. At e14.5, expression of GJA1 was marginal in both the control and mutant animals, with most of the expression detected in the interstitial tissue and only weak expression observed in the testis cords (Figure 5A). A marked increase in the expression of GJA1 was observed in the testis cords of control and mutant animals at e16.5. However, GJA1 expression was more important at the periphery of the testis cords in control animals, a pattern of expression that is not observed in mutant animals (Figure 5A). At e17.5, GJA1 expression was mainly observed at the periphery of testis cords (at the presumed Sertoli cell junctions), while GJA1 expression was lost in the majority of the testis cords of the mutant animals (Figure 5A). Furthermore, the mRNA levels for occludin (*Ocln*), a major contributor to Sertoli cell tight junctions, and for par-6 family cell polarity regulator beta (*Pard6b*), a gene important for apicobasal polarity, also decreased in the testes of mutant animals (Figure 5B) suggesting that epithelization of the Sertoli cells was affected in *Lats1^{flox/flox};Lats2^{flox/flox};Nr5a1-cre* mice.

To further determine if the loss of *Lats1* and *Lats2* in Sertoli cells affects their cellular identity, immunohistochemistry for WT1 and SOX9 was performed. In control animals, WT1+ and SOX9+ positive cells were mostly located at the periphery of the testis cords from e14.5 to 1dpp, though rare positive cells were observed in the middle of the cords at e14.5 (Figure 6A,B). In the testes of mutant animals, an increasing portion of WT1+ was found in the middle of the testis cords between e14.5 and 1dpp (Figure 6A, arrow), again suggesting that these Sertoli cells had lost their polarity. Interestingly, even if localization of SOX9+ cells were initially similar to WT1+ cells in *Lats1^{flox/flox};Lats2^{flox/flox};Nr5a1-cre*, only rare SOX9+ cells could be detected in the seminiferous tubules of 1dpp mice (Figure 6B). To confirm the results obtained by immunohistochemistry and to further characterize the Sertoli cells in *Lats1^{flox/flox};Lats2^{flox/flox};Nr5a1-cre* mice, the expression of the Sertoli cell markers cytochrome P450, 26, retinoic acid B1 (*Cyp26b1*), desert hedgehog (*Dhh*), doublesex and mab-3-related transcription factor 1 (*Dmrt1*), *Sox9*, and *Wt1* were evaluated by RT-qPCR at 1dpp. Interestingly, the mRNA levels of all Sertoli cell markers decreased significantly except for the mRNA levels of *Wt1*, which were maintained in the testes of mutant animals (Figure 6C). To determine if Sertoli cells could differentiate into granulosa cells, RT-qPCR were also performed for forkhead box L2 (*Foxl2*) and wingless-type MMTV integration site family, member 4 (*Wnt4*). However, expression levels of both markers did not increase in the testes of mutant animals (Figure S3). Taken together, the epithelization defect and the expression of Sertoli cell markers suggest that the loss of *Lats1/2* affects the identity of the Sertoli cells but that these cells do not transdifferentiate into granulosa cells.

A- GJA1



B-

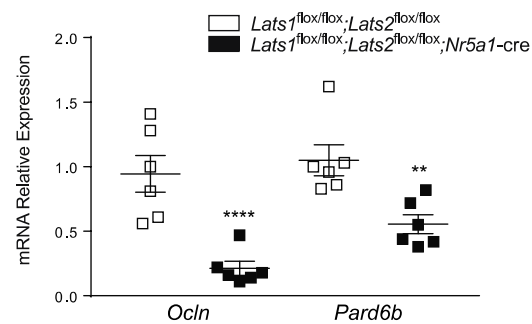


Figure 5. Loss of *Lats1* and *Lats2* affects the polarity of the Sertoli cells. (A) Immunohistochemical analysis of GJA1 expression in testes of mice of the indicated genotypes. Scale bar (lower right) is valid for all images. (B) RT-qPCR analysis of *Ocln* and *Pard6b* mRNA levels in the testes of 1 dpp mice of the indicated genotypes ($n = 6$ animals/genotype). All data were normalized to the housekeeping gene *Rpl19* and are expressed as means (columns) \pm SEM (error bars). Asterisks = significantly different from control (** $p < 0.01$; **** $p < 0.0001$).

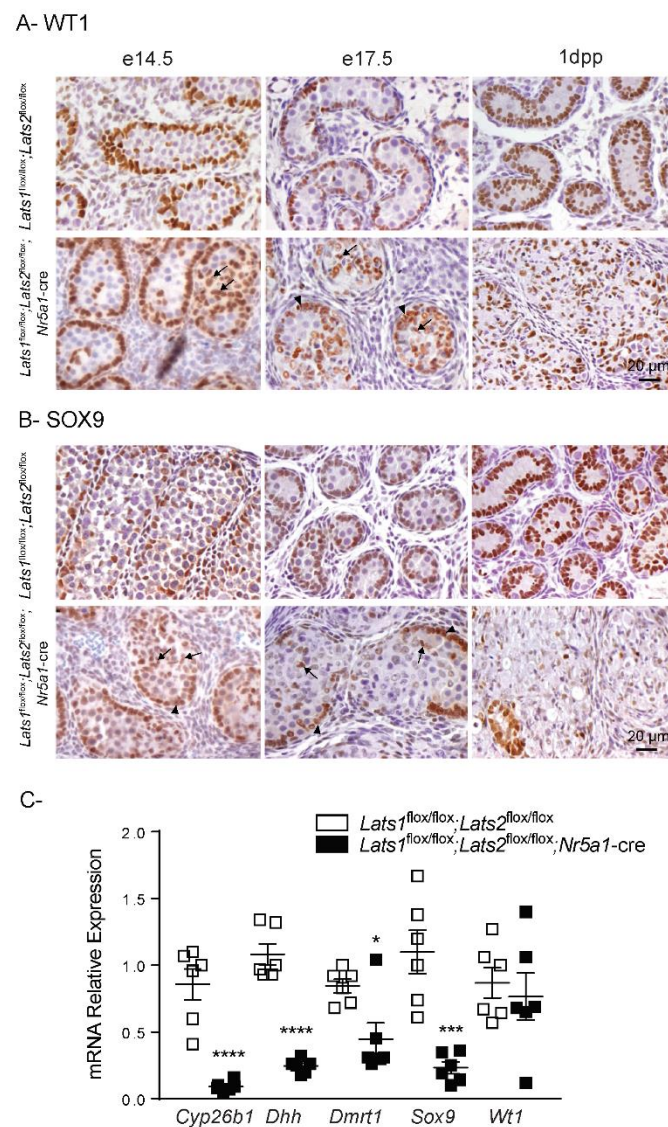


Figure 6. Loss of *Lats1* and *Lats2* affects expression of key Sertoli cell markers. (A) Immunohistochemical analysis of WT1 expression in testes of mice of the indicated genotypes. (B) Immunohistochemical analysis of SOX9 expression in testes of mice of the indicated genotypes. Arrow = immunopositive cells that lost their polarity. Arrowhead = immunopositive cells with normal polarity. Scale bar (lower right) is valid for all images. (C) RT-qPCR analysis of Sertoli cell markers in testes of 1dpp mice of the indicated genotypes ($n = 6$ animals/genotype). All data were normalized to the housekeeping gene *Rpl19* and are expressed as means (columns) \pm SEM (error bars). Asterisks = significantly different from control (* $p < 0.05$; *** $p < 0.001$; **** $p < 0.0001$).

2.5. Disruption of *Lats1* and *Lats2* Causes the Loss of Steroidogenic Markers and Leads to Fibrosis of the Testis Interstitium

To characterize the consequences of *Lats1* and *Lats2* deletion in FLCs, CYP17A1 expression was evaluated by immunohistochemistry. At e14.5, the expression of CYP17A1 was indistinguishable between control and mutant animals (Figure 7A). However, at e17.5, the number of CYP17A1+ cells was considerably reduced in the testes of mutant animals compared to their control counterparts (Figure 7A).

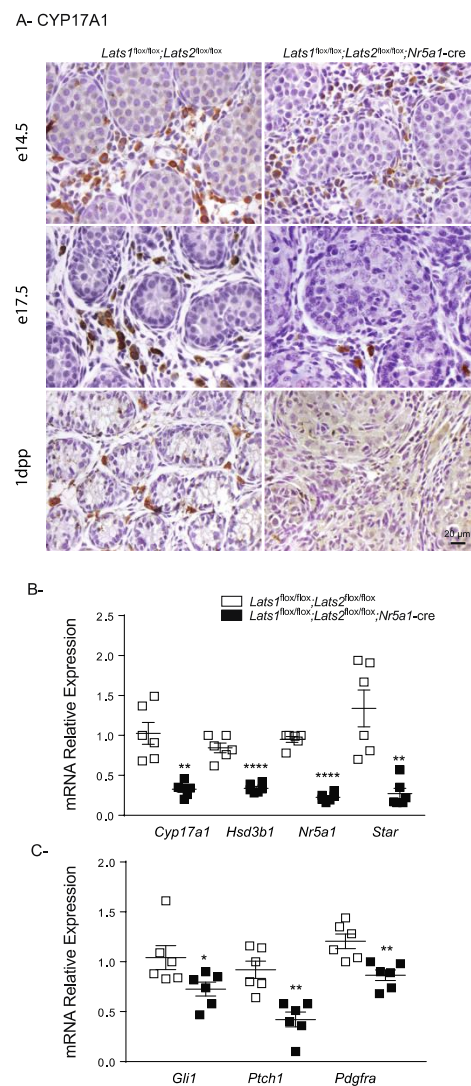


Figure 7. Loss of *Lats1* and *Lats2* affects FLCs. (A) Immunohistochemical analysis of CYP17A1 expression in testes of mice of the indicated genotypes. Scale bar (lower right) is valid for all images. (B,C) RT-qPCR analysis of steroidogenesis (B) and progenitor FLC markers (C) in testes of 1dpp mice of the indicated genotypes ($n = 6$ animals/genotype). All data were normalized to the housekeeping gene *Rpl19* and are expressed as means (columns) \pm SEM (error bars). Asterisks = significantly different from control (* $p < 0.05$; ** $p < 0.01$; **** $p < 0.0001$).

By 1dpp, CYP17A1⁺ cells were completely absent in the testes of mutant animals (Figure 7A). To confirm the loss of steroidogenic cells, *Cyp17a1*, hydroxy-delta-5-steroid dehydrogenase, 3 beta- and steroid-delta-isomerase 1 (*Hsd3b1*), nuclear receptor subfamily 5, group A, member 1 (*Nr5a1*) and steroidogenic acute regulatory protein (*Star*) mRNA levels were evaluated. As expected, a marked loss of every steroidogenic marker was observed in testes of *Lats1*^{fllox/fllox};*Lats2*^{fllox/fllox};*Nr5a1-cre* mice (Figure 7B). Together, these results suggest that like Sertoli cells, FLC differentiation initially occurs but that FLC subsequently lose their steroidogenic capacity.

To further characterize the FLC population, expression of platelet-derived growth factor receptor, alpha polypeptide (*Pdgfra*), and patched homolog 1 (*Ptch1*), which are initially expressed in both interstitial cells and non-steroidogenic FLCs progenitors [49–52], as well as the effector of Hedgehog signaling *Gli1*, were also evaluated by RT-qPCR at 1dpp. Again, a significant decrease in the mRNA levels of all three markers were observed in testes of *Lats1*^{fllox/fllox};*Lats2*^{fllox/fllox};*Nr5a1-cre* mice (Figure 7C), arguing against the possibility that FLCs dedifferentiate into non-steroidogenic FLCs progenitors.

The progressive loss of steroidogenesis and the adoption of a myofibroblast-like spindle shape by the testis interstitial cells was reminiscent of similar changes that occur in the adrenal gland of *Lats1*^{flox/flox};*Lats2*^{flox/flox};*Nr5a1*-cre mice [42]. In the latter, adrenocortical cells (which share a common embryonic origin with FLCs) overexpress the mesenchymal cell and myofibroblast marker vimentin (VIM), followed by an increase in the expression of the myocyte and myofibroblast marker α -SMA [42]. To determine if this was also the case in the testes, VIM and α -SMA expression were evaluated in the testes of control and mutant mice. A marked increase in the number of VIM+ cells was detected in the interstitial tissue of the mutant testes compared to controls (Figure 8A,B) at e17.5. Interestingly, the expression pattern of VIM was also modified in the Sertoli cells (Figure 8A,B). An increase in α -SMA expression was detected in the majority of the interstitial cells of mutant animals (Figure 8C,D) but only at 1dpp. This increase of expression was also associated with an increase in the mRNA levels of actin, alpha 2, smooth muscle, aorta (*Acta2*, the gene coding for α -SMA), and of the myofibroblast markers caldesmon 1 (*Cald1*) and secreted phosphoprotein 1 (*Spp1*) (Figure 8E), as well as with the eventual accumulation of collagen fibers in the interstitial tissue of older animals (Figure 8F, G). Together these results suggest that the transdifferentiation of the FLCs cells could be at least in part responsible for the interstitial fibrosis.

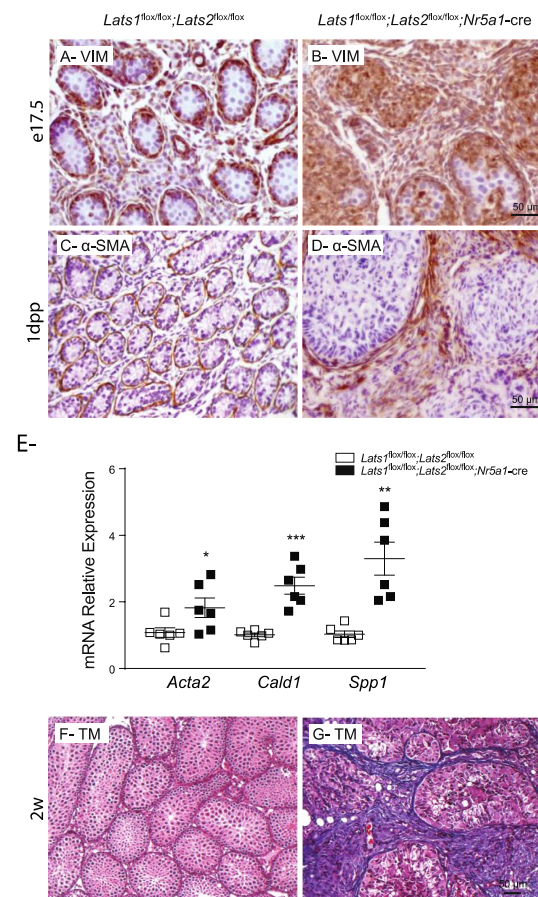


Figure 8. Loss of *Lats1* and *Lats2* leads to fibrosis in the testis interstitial tissue. (A,B) Immunohistochemical analysis of VIM expression in testes of e17.5 mice of the indicated genotypes. (C,D) Immunohistochemical analysis of α -SMA expression in testes of 1dpp mice of the indicated genotypes. (E) RT-qPCR analysis of myofibroblast markers in testes of 1dpp mice of the indicated genotypes ($n = 6$ animals/genotype). All data were normalized to the housekeeping gene *Rpl19* and are expressed as means (columns) \pm SEM (error bars). Asterisks = significantly different from control (* $p < 0.05$; ** $p < 0.01$; *** $p < 0.001$). (F,G) Masson's trichrome staining of 2-week-old mice of the indicated phenotype. Scale bars in the right panels are valid for the left panels.

3. Discussion

In recent years, Hippo has been identified as one of the most important signaling pathways involved in tissue development; however, no study has evaluated its function in the development of the testes. We report herein that the concomitant inactivation of the two core kinases of the Hippo pathway, *Lats1* and *Lats2*, alters the fate of the testicular somatic cells.

Even though NR5A1 is normally expressed early during gonadal development (e9.5–10.0) in a progenitor cell population that differentiate into both Sertoli cells and FLCs [13], the loss of *Lats1/2* observed in the *Lats1^{flox/flox};Lats2^{flox/flox};Nr5a1-cre* model was only apparent in late stages of testis development, as suggested by the loss of *Lats1* and *Lats2* mRNA levels and concomitant loss of YAP phosphorylation. This result could be explained in one of two ways. First, it is possible that recombination of the *Lats1* and *Lats2* floxed alleles is not efficient in testis somatic cells. Second, it is possible that the *Nr5a1-cre* model used in the present study does not sufficiently express Cre in the early stages of testis development to allow proper recombination. In that regard, it is important to note that the *Nr5a1-cre* model used for this study was the one developed by the Lowell group [41], which has never been fully characterized in the early stages of testis development and which has been used more sparingly than the model developed by the Parker group [53]. No matter the reason, our results suggest that efficient recombination only occurs when Sertoli cells and FLCs are already committed to their respective lineage, and it can be concluded that the phenotypic changes observed in the mutants herein are most likely due to the transdifferentiation of the Sertoli cells and FLCs rather than to the altered differentiation of their common progenitors.

Inactivation of *Lats1/2* seems to impair the development of both Sertoli cells and FLCs cells in the *Lats1^{flox/flox};Lats2^{flox/flox};Nr5a1-cre* animals. In Sertoli cells, the redistribution/increase of VIM expression, the absence of increase in junction protein, alpha 1, 43 KDA (GJA1) expression, the decrease in the expression of *Ocln* and *Pard6b*, and the presence of WT1+ and SOX9+ cells at the center of the tubules together suggest that Sertoli cells lose their epithelial nature and potentially gain characteristics of mesenchymal cells in mutant mice. Epithelial–mesenchymal transition (EMT) is a common event following the downregulation of Hippo signaling and the increase in YAP/TAZ activity [39,54–59] and has notably been reported to occur in ovarian granulosa cells [39], which share a common precursor with Sertoli cells [4]. Interestingly, it was shown that YAP and WT1 act in synergy to loosen cell–cell contacts and trigger EMT in the epithelial MDCK cell line [59], suggesting that YAP or TAZ could act with WT1 in a similar manner in Sertoli cells. It was also previously observed that Sertoli cells initially have mesenchyme-like behaviors and morphology before migrating to the periphery of the testis cords and gaining characteristics of epithelial cells [60]. The phenotype observed in the *Lats1^{flox/flox};Lats2^{flox/flox};Nr5a1-cre* model could therefore suggest that the Sertoli cells regain characteristics of mesenchymal cells and dedifferentiate to a more primitive stage of development. The fact that WT1 expression (whose expression precedes the differentiation of the Sertoli cell expression [16,61,62]) is maintained in the majority of the presumptive Sertoli cells while SOX9 and *Dhh* are lost also argues in favor of the dedifferentiation of the Sertoli cells. Further experiments are required to delineate the role of Hippo signaling in the maintenance of the identity of the Sertoli cells.

Loss of SOX9 expression in the presumptive immature Sertoli cells of the *Lats1^{flox/flox};Lats2^{flox/flox};Nr5a1-cre* animals was surprising as it was previously shown that loss of *Yap* and *Taz* leads to the downregulation of SOX9 expression in primary cultures of immature Sertoli cells [38] and that loss of *Lats1* and *Lats2* in postnatal granulosa cells leads to an increase in SOX9 expression and the appearance of Sertoli-like cells in the ovary [39]. This finding suggests that interactions between Hippo signaling and *Sox9* expression are more complex than expected. Since YAP and TAZ can bind several transcription factors, it is possible that the presence or absence of other transcription factors during different stages of Sertoli cell development dictate the regulation of *Sox9* by Hippo signaling. Another possibility is that very tight regulation of the transcriptional activity of YAP and TAZ is

necessary to direct proper levels of *Sox9* expression and to determine Sertoli cell fate. For instance, basal levels of YAP and TAZ expression may be necessary for proper expression of SOX9 in the developing Sertoli cells, while overexpression of YAP and TAZ could lead to its inactivation. Indeed, a phenomenon similar to this has been reported to occur in the developing kidney, where the deletion of *Yap* in the cap mesenchyme prevents nephron formation [63], whereas the overexpression of YAP/TAZ leads to the differentiation of nephron progenitors into myofibroblasts [64].

Aside from the Sertoli cells, the interstitial tissues were also affected in the *Lats1^{flox/flox};Lats2^{flox/flox};Nr5a1-cre* animals. Loss of steroidogenic FLCs and the concomitant appearance of a spindle-shaped cell population leading to the development of interstitial fibrosis was observed in the testis of mutant animals at e16.5. Because steroidogenic cells progressively transdifferentiate into myofibroblast-like cells in the adrenal cortex of *Lats1^{flox/flox};Lats2^{flox/flox};Nr5a1-cre* animals [42], we hypothesized that FLCs (which share a common origin with the steroidogenic cells of the adrenal cortex) also transdifferentiate into myofibroblast-like cells in these animals. Interestingly, it was previously shown that disruption of *Nr5a1* in FLCs leads to massive interstitial fibrosis caused by the synthesis of extracellular matrix by the *Nr5a1*-disrupted FLCs [65], suggesting that loss of *Nr5a1* in our model could be responsible for the observed fibrosis. Though it seems likely that some myofibroblast-like cells were of Leydig cell origin, we cannot rule out the possibility that others originated from peritubular myoid cells or other stromal cell types. Lineage tracing experiments would be needed to determine their origin unequivocally. Hippo signaling inactivation and YAP/TAZ transcriptional activation have also been shown to play a major roles in the transdifferentiation of cells into myofibroblasts and fibrosis in non-endocrine tissues such as the lung [66] and the heart [67] as well as in tissues derived from the intermediate mesoderm such as the kidney [68] and the Mullerian duct [69]. Among the known downstream targets of YAP/TAZ, CTGF could play an important role in the transdifferentiation of FLCs into myofibroblast-like cells. Indeed, CTGF has been previously described as a key driver of fibrosis [70–73] and myofibroblast formation [74–76]. Furthermore, it was shown that TAZ was dramatically enriched on the promoter of *Ctgf* following inactivation of *Lats1/2* in mouse Mullerian ducts, leading to *Ctgf* overexpression and myofibroblast transdifferentiation [69].

Even though we attributed the phenotypic changes observed in the Sertoli cells and FLCs of *Lats1^{flox/flox};Lats2^{flox/flox};Nr5a1-cre* mice to the direct loss of *Lats1/2* in these cell types, there is also a possibility that the loss of *Lats1/2* in Sertoli cells affected the FLCs and vice versa. For example, loss of DHH secretion by Sertoli cells in *Lats1^{flox/flox};Lats2^{flox/flox};Nr5a1-cre* animals could affect FLC differentiation [11]. Conversely, loss of Activin A secretion by FLCs could indirectly affect Sertoli cells and testis cord formation [77]. Activin A increases SOX9 nuclear localization in the esophageal adenocarcinoma cell line FLO-1 [78], suggesting that Activin A could also regulate SOX9 in the Sertoli cells. Furthermore, transdifferentiation of the FLC population into myofibroblast-like cells could mechanically interfere with testis cord development. In agreement with this hypothesis, it was shown that inactivation of *Lats1/2* in the Müllerian duct mesenchyme cells prior to the degradation of the Müllerian ducts in males leads to their differentiation into myofibroblasts, which in turn interfere with the development and the coiling of the adjacent epididymides [69]. Transgenic models that target *Lats1/2* specifically in the Sertoli cells and the FLCs are needed to distinguish between the direct and indirect effects in each cell population. Lastly, though an increase in YAP/TAZ transcriptional activity in the testes of *Lats1^{flox/flox};Lats2^{flox/flox};Nr5a1-cre* animals is the presumptive driving force behind the observed phenotypic changes, it is important to mention that LATS1/2 can occasionally act independently of the canonical Hippo pathway [79,80]. The generation of a *Lats1^{flox/flox};Lats2^{flox/flox};Yap^{flox/flox};Taz^{flox/flox};Nr5a1-cre* mouse model is needed to determine if YAP/TAZ stabilization is solely responsible for the effects of *Lats1/2* loss.

In summary, we report here a previously unheard role of the Hippo pathway in the development of the testis, as loss of *Lats1/2* results in testis cord dysgenesis and interstitial

fibrosis. Further studies are required to define the mechanism of action of Hippo signaling throughout testis development in both FLC and Sertoli cell differentiation.

4. Material and Methods

4.1. Ethics

Animal procedures were approved by the Comité d'Éthique de l'Utilisation des Animaux of the Université de Montréal (protocol numbers Rech-1739 and Rech-1909 respectively approved in 2015 and 2017) and conformed to the guidelines of the Canadian Council on Animal Care.

4.2. Transgenic Mouse Strains

Nr5a1-cre mice (FVB-Tg-*Nr5a1*^{Cre7Low1/J}) were obtained from the Jackson Laboratory and maintained by crossing Cre-positive males with wild-type females (C57BL/6J). *Lats1*^{flox/flox} (*Lats1*^{tm1.1JFm/RjoJ}) and *Lats2*^{flox/flox} (*Lats2*^{tm1.1JFm/RjoJ}) mice were obtained from Dr. Randy L. Johnson (M.D. Anderson Cancer Center, Houston, TX, USA). Mice were selectively bred over several generations to obtain the *Lats1*^{flox/flox};*Nr5a1*-cre, *Lats2*^{flox/flox};*Nr5a1*-cre and *Lats1*^{flox/flox};*Lats2*^{flox/flox};*Nr5a1*-cre genotypes. Genotype analyses were done on tail biopsies by PCR as previously described for Cre [41] and *Lats1/2* [81].

4.3. Tissue Collection

All embryos or testes were collected from e12.5 to e17.5, 1dpp (day post-partum) and 2-week-old *Lats1*^{flox/flox};*Lats2*^{flox/flox};*Nr5a1*-cre male mice and *Lats1*^{flox/flox};*Lats2*^{flox/flox} control littermates and were fixed in 4% paraformaldehyde for 4 h (whole embryos, 1 dpp testes) or Bouin's fixative overnight (testes from 2-week-old mice) and embedded in paraffin for histopathologic analyses or immunohistochemistry (IHC). Some testes from e14.5, e17.5, and 1dpp animals were flash frozen followed by homogenization for quantitative RT-PCR (RT-qPCR).

4.4. Histopathology and Immunohistochemistry

Histopathology analyses were performed on paraffin embedded, 5 µm thick tissues stained with hematoxylin and eosin (H&E) or Masson's trichrome. Immunohistochemistry analyses were performed on paraffin-embedded, 5 µm thick tissue sections using VectaStain Elite avidin-biotin complex method kits (Vector Laboratories, Newark, CA, USA) or mouse on mouse (M.O.M.) elite peroxidase kit (Vector Laboratories) as directed by the manufacturers. Sections were probed with antibodies against cCASP3, CYP17A1, DDX4, GJA1, α-SMA, SOX9, TAZ, VIM, WT1, YAP, or phospho-YAP. Staining was done using the 3,3'-diaminobenzidine peroxidase substrate kit (Vector Laboratories) or with a chromogen (Agilent) and counterstained with hematoxylin before mounting. Negative controls consisted of slides for which the primary antibody was omitted. Antibodies used are listed in Supplemental Table S1.

4.5. Reverse-Transcription-Quantitative PCR

Total RNA from testes of e14.5, e17.5, and 1 dpp animals was extracted using the Total RNA Mini Kit (FroggaBio, Concord, ON, Canada) according to the manufacturer's protocol. Total RNA was reverse-transcribed using 100 ng of RNA and the SuperScriptVilo™ cDNA synthesis kit (Thermo Fisher scientific, Waltham, Ma, U.S.). Real-time PCR reactions were run on a CFX96 Touch instrument (Bio-Rad, Hercules, CA, USA), using Supergreen Advanced qPCR MasterMix (Wisent, St-Bruno, Qc, Canada). Each PCR reaction consisted of 7.5 µL of Power SYBR Green PCR Master Mix, 2.3 µL of water, 4 µL of cDNA sample and 0.6 µL (400 nmol) of gene-specific primers. PCR reactions run without cDNA (water blank) served as negative controls. A common thermal cycling program (3 min at 95 °C, m of 15 s at 95 °C, 30 s at 60 °C and 30 s at 72 °C) was used to amplify each transcript. To quantify relative gene expression, the Ct of genes of interest was compared with that of *Rpl19*, according to the ratio $R = [E^{Ct_{Rpl19}} / E^{Ct_{target}}]$ where E is the amplification efficiency

for each primer pair. *Rpl19* Ct values did not change significantly between tissues, and *Rpl19* was therefore deemed suitable as an internal reference gene. The specific primer sequences used are listed in Supplemental Table S2.

4.6. Statistical Analyses

All statistical analyses were performed with Prism software version 6.0d (GraphPad Software Inc., CA, USA, RRID: SCR_002798). All the datasets were subjected to the *F* test to determine the equality of variances. Student's *t*-test was used for all comparisons between genotypes. Means were considered significantly different when *p* value was < 0.05. All data are presented as means \pm SEM.

Supplementary Materials: The following supporting information can be downloaded at: <https://www.mdpi.com/article/10.3390/ijms232113585/s1>.

Author Contributions: N.A.N. performed most of the experiments described in this manuscript, analyzed the data, and wrote the first draft of the manuscript. A.M., A.L., and G.S.-J. helped to perform some experiments. G.Z. and D.B. provided supervision to trainees and manuscript revision. A.B. conceived and designed the experiments, supervised trainees, and wrote the final draft of the manuscript. All authors have read and agreed to the published version of the manuscript.

Funding: This work was supported by Discovery Grants and an accelerator supplement (RGPIN-2020-05230 and RGPAS-2020-00026 to AB) a Discovery grant (RGPIN-2018-06470 to GZ) from the Natural Sciences and Engineering Research Council of Canada (NSERC). NAN is a recipient of a PhD scholarship from the Fonds de Recherche Québec—Nature et technologies (FRQNT). AM is a recipient of a graduate scholarship from NSERC.

Institutional Review Board Statement: Animal procedures were approved by the Comité d'Éthique de l'Utilisation des Animaux of the Université de Montréal (protocol numbers Rech-1739 and Rech-1909) and conformed to the guidelines of the Canadian Council on Animal Care.

Informed Consent Statement: Not applicable.

Data Availability Statement: All relevant data are within the paper and its supporting information files.

Acknowledgments: The authors would like to thank Manon Salvat, Marie LeGad-LeRoy, and Nadia Ménard for technical assistance and Randy L. Johnson (M.D. Anderson Cancer Center, Houston Tx) for generously providing the *Lats1/2* floxed mice.

Conflicts of Interest: The authors have no conflicts of interest to declare.

References

1. Hatano, O.; Takakusu, A.; Nomura, M.; Morohashi, K. Identical origin of adrenal cortex and gonad revealed by expression profiles of Ad4BP/SF-1. *Genes Cells* **1996**, *1*, 663–671. [[CrossRef](#)] [[PubMed](#)]
2. Bandiera, R.; Sacco, S.; Vidal, V.P.; Chaboissier, M.C.; Schedl, A. Steroidogenic organ development and homeostasis: A WT1-centric view. *Mol. Cell. Endocrinol.* **2015**, *408*, 145–155. [[CrossRef](#)] [[PubMed](#)]
3. Val, P.; Martinez-Barbera, J.P.; Swain, A. Adrenal development is initiated by Cited2 and Wt1 through modulation of Sf-1 dosage. *Development* **2007**, *134*, 2349–2358. [[CrossRef](#)] [[PubMed](#)]
4. Albrecht, K.H.; Eicher, E.M. Evidence that Sry is expressed in pre-Sertoli cells and Sertoli and granulosa cells have a common precursor. *Dev. Biol.* **2001**, *240*, 92–107. [[CrossRef](#)]
5. Schmahl, J.; Eicher, E.M.; Washburn, L.L.; Capel, B. Sry induces cell proliferation in the mouse gonad. *Development* **2000**, *127*, 65–73. [[CrossRef](#)]
6. Chaboissier, M.C.; Kobayashi, A.; Vidal, V.I.; Lützkendorf, S.; van de Kant, H.J.; Wegner, M.; de Rooij, D.G.; Behringer, R.R.; Schedl, A. Functional analysis of Sox8 and Sox9 during sex determination in the mouse. *Development* **2004**, *131*, 1891–1901. [[CrossRef](#)]
7. Kim, Y.; Kobayashi, A.; Sekido, R.; DiNapoli, L.; Brennan, J.; Chaboissier, M.C.; Poulat, F.; Behringer, R.R.; Lovell-Badge, R.; Capel, B. Fgf9 and Wnt4 act as antagonistic signals to regulate mammalian sex determination. *PLoS Biol.* **2006**, *4*, e187. [[CrossRef](#)]
8. Schmahl, J.; Kim, Y.; Colvin, J.S.; Ornitz, D.M.; Capel, B. Fgf9 induces proliferation and nuclear localization of FGFR2 in Sertoli precursors during male sex determination. *Development* **2004**, *131*, 3627–3636. [[CrossRef](#)]
9. Clark, A.M.; Garland, K.K.; Russell, L.D. Desert hedgehog (Dhh) gene is required in the mouse testis for formation of adult-type Leydig cells and normal development of peritubular cells and seminiferous tubules. *Biol. Reprod.* **2000**, *63*, 1825–1838. [[CrossRef](#)]

10. Pierucci-Alves, F.; Clark, A.M.; Russell, L.D. A developmental study of the Desert hedgehog-null mouse testis. *Biol. Reprod.* **2001**, *65*, 1392–1402. [[CrossRef](#)]
11. Yao, H.H.; Whoriskey, W.; Capel, B. Desert Hedgehog/Patched 1 signaling specifies fetal Leydig cell fate in testis organogenesis. *Genes Dev.* **2002**, *16*, 1433–1440. [[CrossRef](#)] [[PubMed](#)]
12. Liu, C.; Rodriguez, K.; Yao, H.H. Mapping lineage progression of somatic progenitor cells in the mouse fetal testis. *Development* **2016**, *143*, 3700–3710. [[CrossRef](#)] [[PubMed](#)]
13. Stévant, I.; Neirijnck, Y.; Borel, C.; Escoffier, J.; Smith, L.B.; Antonarakis, S.E.; Dermitzakis, E.T.; Nef, S. Deciphering Cell Lineage Specification during Male Sex Determination with Single-Cell RNA Sequencing. *Cell Rep.* **2018**, *22*, 1589–1599. [[CrossRef](#)]
14. Stévant, I.; Kühne, F.; Greenfield, A.; Chaboissier, M.C.; Dermitzakis, E.T.; Nef, S. Dissecting Cell Lineage Specification and Sex Fate Determination in Gonadal Somatic Cells Using Single-Cell Transcriptomics. *Cell Rep.* **2019**, *26*, 3272–3283.e3273. [[CrossRef](#)] [[PubMed](#)]
15. Shimamura, R.; Fraizer, G.C.; Trapman, J.; Lau Yf, C.; Saunders, G.F. The Wilms' tumor gene WT1 can regulate genes involved in sex determination and differentiation: SRY, Müllerian-inhibiting substance, and the androgen receptor. *Clin. Cancer Res.* **1997**, *3*, 2571–2580.
16. Bradford, S.T.; Wilhelm, D.; Bandiera, R.; Vidal, V.; Schedl, A.; Koopman, P. A cell-autonomous role for WT1 in regulating Sry in vivo. *Hum. Mol. Genet.* **2009**, *18*, 3429–3438. [[CrossRef](#)] [[PubMed](#)]
17. Wen, Q.; Zheng, Q.S.; Li, X.X.; Hu, Z.Y.; Gao, F.; Cheng, C.Y.; Liu, Y.X. Wt1 dictates the fate of fetal and adult Leydig cells during development in the mouse testis. *Am. J. Physiol. Endocrinol. Metab.* **2014**, *307*, E1131–E1143. [[CrossRef](#)]
18. Zhang, L.; Chen, M.; Wen, Q.; Li, Y.; Wang, Y.; Wang, Y.; Qin, Y.; Cui, X.; Yang, L.; Huff, V.; et al. Reprogramming of Sertoli cells to fetal-like Leydig cells by Wt1 ablation. *Proc. Natl. Acad. Sci. USA* **2015**, *112*, 4003–4008. [[CrossRef](#)]
19. Luo, X.; Ikeda, Y.; Parker, K.L. A cell-specific nuclear receptor is essential for adrenal and gonadal development and sexual differentiation. *Cell* **1994**, *77*, 481–490. [[CrossRef](#)]
20. Tevosian, S.G.; Albrecht, K.H.; Crispino, J.D.; Fujiwara, Y.; Eicher, E.M.; Orkin, S.H. Gonadal differentiation, sex determination and normal Sry expression in mice require direct interaction between transcription partners GATA4 and FOG2. *Development* **2002**, *129*, 4627–4634. [[CrossRef](#)]
21. Hu, Y.C.; Okumura, L.M.; Page, D.C. Gata4 is required for formation of the genital ridge in mice. *PLoS Genet.* **2013**, *9*, e1003629. [[CrossRef](#)] [[PubMed](#)]
22. Viger, R.S.; de Mattos, K.; Tremblay, J.J. Insights Into the Roles of GATA Factors in Mammalian Testis Development and the Control of Fetal Testis Gene Expression. *Front. Endocrinol.* **2022**, *13*, 902198. [[CrossRef](#)] [[PubMed](#)]
23. Nef, S.; Verma-Kurvari, S.; Merenmies, J.; Vassalli, J.D.; Efstratiadis, A.; Accili, D.; Parada, L.F. Testis determination requires insulin receptor family function in mice. *Nature* **2003**, *426*, 291–295. [[CrossRef](#)] [[PubMed](#)]
24. Pitetti, J.L.; Calvel, P.; Romero, Y.; Conne, B.; Truong, V.; Papaioannou, M.D.; Schaad, O.; Docquier, M.; Herrera, P.L.; Wilhelm, D.; et al. Insulin and IGF1 receptors are essential for XX and XY gonadal differentiation and adrenal development in mice. *PLoS Genet.* **2013**, *9*, e1003160. [[CrossRef](#)]
25. Fujimoto, Y.; Tanaka, S.S.; Yamaguchi, Y.L.; Kobayashi, H.; Kuroki, S.; Tachibana, M.; Shinomura, M.; Kanai, Y.; Morohashi, K.; Kawakami, K.; et al. Homeoproteins Six1 and Six4 regulate male sex determination and mouse gonadal development. *Dev. Cell* **2013**, *26*, 416–430. [[CrossRef](#)]
26. Garcia-Moreno, S.A.; Lin, Y.T.; Futtner, C.R.; Salamone, I.M.; Capel, B.; Maatouk, D.M. CBX2 is required to stabilize the testis pathway by repressing Wnt signaling. *PLoS Genet.* **2019**, *15*, e1007895. [[CrossRef](#)]
27. Katoh-Fukui, Y.; Miyabayashi, K.; Komatsu, T.; Owaki, A.; Baba, T.; Shima, Y.; Kidokoro, T.; Kanai, Y.; Schedl, A.; Wilhelm, D.; et al. Cbx2, a polycomb group gene, is required for Sry gene expression in mice. *Endocrinology* **2012**, *153*, 913–924. [[CrossRef](#)]
28. Maugeri-Sacca, M.; De Maria, R. The Hippo pathway in normal development and cancer. *Pharmacol. Ther.* **2018**, *186*, 60–72. [[CrossRef](#)]
29. Piccolo, S.; Dupont, S.; Cordenonsi, M. The biology of YAP/TAZ: Hippo signaling and beyond. *Physiol. Rev.* **2014**, *94*, 1287–1312. [[CrossRef](#)]
30. Hong, A.W.; Meng, Z.; Yuan, H.X.; Plouffe, S.W.; Moon, S.; Kim, W.; Jho, E.H.; Guan, K.L. Osmotic stress-induced phosphorylation by NLK at Ser128 activates YAP. *EMBO Rep.* **2017**, *18*, 72–86. [[CrossRef](#)]
31. Moon, S.; Kim, W.; Kim, S.; Kim, Y.; Song, Y.; Bilousov, O.; Kim, J.; Lee, T.; Cha, B.; Kim, M.; et al. Phosphorylation by NLK inhibits YAP-14-3-3-interactions and induces its nuclear localization. *EMBO Rep.* **2017**, *18*, 61–71. [[CrossRef](#)] [[PubMed](#)]
32. Wehling, L.; Keegan, L.; Fernández-Palanca, P.; Hassan, R.; Ghallab, A.; Schmitt, J.; Schirmacher, P.; Kummer, U.; Hengstler, J.G.; Sahle, S.; et al. Spatial modeling reveals nuclear phosphorylation and subcellular shuttling of YAP upon drug-induced liver injury. *bioRxiv* **2022**. [[CrossRef](#)]
33. Li, W.; Cooper, J.; Zhou, L.; Yang, C.; Erdjument-Bromage, H.; Zagzag, D.; Snuderl, M.; Ladanyi, M.; Hanemann, C.O.; Zhou, P.; et al. Merlin/NF2 loss-driven tumorigenesis linked to CRL4(DCAF1)-mediated inhibition of the hippo pathway kinases Lats1 and 2 in the nucleus. *Cancer Cell* **2014**, *26*, 48–60. [[CrossRef](#)] [[PubMed](#)]
34. Varelas, X. The Hippo pathway effectors TAZ and YAP in development, homeostasis and disease. *Development* **2014**, *141*, 1614–1626. [[CrossRef](#)]
35. Sen Sharma, S.; Majumdar, S.S. Transcriptional co-activator YAP regulates cAMP signaling in Sertoli cells. *Mol. Cell. Endocrinol.* **2017**, *450*, 64–73. [[CrossRef](#)]

36. Sen Sharma, S.; Vats, A.; Majumdar, S. Regulation of Hippo pathway components by FSH in testis. *Reprod. Biol.* **2019**, *19*, 61–66. [[CrossRef](#)]
37. Badr, G.; Abdel-Tawab, H.S.; Ramadan, N.K.; Ahmed, S.F.; Mahmoud, M.H. Protective effects of camel whey protein against scrotal heat-mediated damage and infertility in the mouse testis through YAP/Nrf2 and PPAR-gamma signaling pathways. *Mol. Reprod. Dev.* **2018**, *85*, 505–518. [[CrossRef](#)]
38. Levasseur, A.; Paquet, M.; Boerboom, D.; Boyer, A. Yes-associated protein and WW-containing transcription regulator 1 regulate the expression of sex-determining genes in Sertoli cells, but their inactivation does not cause sex reversal. *Biol. Reprod.* **2017**, *97*, 162–175. [[CrossRef](#)]
39. Tsoi, M.; Morin, M.; Rico, C.; Johnson, R.L.; Paquet, M.; Gévry, N.; Boerboom, D. Lats1 and Lats2 are required for ovarian granulosa cell fate maintenance. *FASEB J.* **2019**, *33*, 10819–10832. [[CrossRef](#)]
40. Chi, X.; Luo, W.; Song, J.; Li, B.; Su, T.; Yu, M.; Wang, T.; Wang, Z.; Liu, C.; Li, Z.; et al. Kindlin-2 in Sertoli cells is essential for testis development and male fertility in mice. *Cell Death Dis.* **2021**, *12*, 604. [[CrossRef](#)]
41. Dhillon, H.; Zigman, J.M.; Ye, C.; Lee, C.E.; McGovern, R.A.; Tang, V.; Kenny, C.D.; Christiansen, L.M.; White, R.D.; Edelstein, E.A.; et al. Leptin directly activates SF1 neurons in the VMH, and this action by leptin is required for normal body-weight homeostasis. *Neuron* **2006**, *49*, 191–203. [[CrossRef](#)] [[PubMed](#)]
42. Ménard, A.; Abou Nader, N.; Levasseur, A.; St-Jean, G.; Le Roy, M.L.G.; Boerboom, D.; Benoit-Biancamano, M.O.; Boyer, A. Targeted Disruption of Lats1 and Lats2 in Mice Impairs Adrenal Cortex Development and Alters Adrenocortical Cell Fate. *Endocrinology* **2020**, *161*, bqaa052. [[CrossRef](#)] [[PubMed](#)]
43. Ikeda, Y.; Shen, W.H.; Ingraham, H.A.; Parker, K.L. Developmental expression of mouse steroidogenic factor-1, an essential regulator of the steroid hydroxylases. *Mol. Endocrinol.* **1994**, *8*, 654–662. [[CrossRef](#)] [[PubMed](#)]
44. Kalluri, R.; Neilson, E.G. Epithelial-mesenchymal transition and its implications for fibrosis. *J. Clin. Investig.* **2003**, *112*, 1776–1784. [[CrossRef](#)]
45. Marconi, G.D.; Fonticoli, L.; Rajan, T.S.; Pierdomenico, S.D.; Trubiani, O.; Pizzicannella, J.; Diomede, F. Epithelial-Mesenchymal Transition (EMT): The Type-2 EMT in Wound Healing, Tissue Regeneration and Organ Fibrosis. *Cells* **2021**, *10*, 1587. [[CrossRef](#)] [[PubMed](#)]
46. Nieto, M.A.; Huang, R.Y.; Jackson, R.A.; Thiery, J.P. EMT: 2016. *Cell* **2016**, *166*, 21–45. [[CrossRef](#)]
47. Carette, D.; Weider, K.; Gilleron, J.; Giese, S.; Dompierre, J.; Bergmann, M.; Brehm, R.; Denizot, J.P.; Segretain, D.; Pointis, G. Major involvement of connexin 43 in seminiferous epithelial junction dynamics and male fertility. *Dev. Biol.* **2010**, *346*, 54–67. [[CrossRef](#)]
48. Sridharan, S.; Simon, L.; Meling, D.D.; Cyr, D.G.; Gutstein, D.E.; Fishman, G.I.; Guillou, F.; Cooke, P.S. Proliferation of adult sertoli cells following conditional knockout of the Gap junctional protein GJA1 (connexin 43) in mice. *Biol. Reprod.* **2007**, *76*, 804–812. [[CrossRef](#)]
49. Inoue, M.; Shima, Y.; Miyabayashi, K.; Tokunaga, K.; Sato, T.; Baba, T.; Ohkawa, Y.; Akiyama, H.; Suyama, M.; Morohashi, K. Isolation and Characterization of Fetal Leydig Progenitor Cells of Male Mice. *Endocrinology* **2016**, *157*, 1222–1233. [[CrossRef](#)]
50. McClelland, K.S.; Bell, K.; Larney, C.; Harley, V.R.; Sinclair, A.H.; Oshlack, A.; Koopman, P.; Bowles, J. Purification and Transcriptomic Analysis of Mouse Fetal Leydig Cells Reveals Candidate Genes for Specification of Gonadal Steroidogenic Cells. *Biol. Reprod.* **2015**, *92*, 145. [[CrossRef](#)]
51. Brennan, J.; Tilmann, C.; Capel, B. Pdgfr-alpha mediates testis cord organization and fetal Leydig cell development in the XY gonad. *Genes Dev.* **2003**, *17*, 800–810. [[CrossRef](#)]
52. Karl, J.; Capel, B. Sertoli cells of the mouse testis originate from the coelomic epithelium. *Dev. Biol.* **1998**, *203*, 323–333. [[CrossRef](#)]
53. Bingham, N.C.; Verma-Kurvari, S.; Parada, L.F.; Parker, K.L. Development of a steroidogenic factor 1/Cre transgenic mouse line. *Genesis* **2006**, *44*, 419–424. [[CrossRef](#)]
54. Xie, D.; Cui, J.; Xia, T.; Jia, Z.; Wang, L.; Wei, W.; Zhu, A.; Gao, Y.; Xie, K.; Quan, M. Hippo transducer TAZ promotes epithelial mesenchymal transition and supports pancreatic cancer progression. *Oncotarget* **2015**, *6*, 35949–35963. [[CrossRef](#)] [[PubMed](#)]
55. Li, S.; Zhang, X.; Zhang, R.; Liang, Z.; Liao, W.; Du, Z.; Gao, C.; Liu, F.; Fan, Y.; Hong, H. Hippo pathway contributes to cisplatin resistant-induced EMT in nasopharyngeal carcinoma cells. *Cell Cycle* **2017**, *16*, 1601–1610. [[CrossRef](#)] [[PubMed](#)]
56. Lei, Q.Y.; Zhang, H.; Zhao, B.; Zha, Z.Y.; Bai, F.; Pei, X.H.; Zhao, S.; Xiong, Y.; Guan, K.L. TAZ promotes cell proliferation and epithelial-mesenchymal transition and is inhibited by the hippo pathway. *Mol. Cell. Biol.* **2008**, *28*, 2426–2436. [[CrossRef](#)]
57. Shao, D.D.; Xue, W.; Krall, E.B.; Bhutkar, A.; Piccioni, F.; Wang, X.; Schinzel, A.C.; Sood, S.; Rosenbluh, J.; Kim, J.W.; et al. KRAS and YAP1 converge to regulate EMT and tumor survival. *Cell* **2014**, *158*, 171–184. [[CrossRef](#)] [[PubMed](#)]
58. Liu, Y.; He, K.; Hu, Y.; Guo, X.; Wang, D.; Shi, W.; Li, J.; Song, J. YAP modulates TGF-beta1-induced simultaneous apoptosis and EMT through upregulation of the EGF receptor. *Sci. Rep.* **2017**, *7*, 45523. [[CrossRef](#)] [[PubMed](#)]
59. Park, J.; Kim, D.H.; Shah, S.R.; Kim, H.N.; Kshitz; Kim, P.; Quinones-Hinojosa, A.; Levchenko, A. Switch-like enhancement of epithelial-mesenchymal transition by YAP through feedback regulation of WT1 and Rho-family GTPases. *Nat. Commun.* **2019**, *10*, 2797. [[CrossRef](#)] [[PubMed](#)]
60. Nel-Themaat, L.; Jang, C.W.; Stewart, M.D.; Akiyama, H.; Viger, R.S.; Behringer, R.R. Sertoli cell behaviors in developing testis cords and postnatal seminiferous tubules of the mouse. *Biol. Reprod.* **2011**, *84*, 342–350. [[CrossRef](#)]
61. Armstrong, J.F.; Pritchard-Jones, K.; Bickmore, W.A.; Hastie, N.D.; Bard, J.B. The expression of the Wilms' tumour gene, WT1, in the developing mammalian embryo. *Mech. Dev.* **1993**, *40*, 85–97. [[CrossRef](#)]

62. Kreidberg, J.A.; Sariola, H.; Loring, J.M.; Maeda, M.; Pelletier, J.; Housman, D.; Jaenisch, R. WT-1 is required for early kidney development. *Cell* **1993**, *74*, 679–691. [[CrossRef](#)]
63. Reginensi, A.; Scott, R.P.; Gregorieff, A.; Bagherie-Lachidan, M.; Chung, C.; Lim, D.S.; Pawson, T.; Wrana, J.; McNeill, H. Yap and Cdc42-dependent nephrogenesis and morphogenesis during mouse kidney development. *PLoS Genet.* **2013**, *9*, e1003380. [[CrossRef](#)] [[PubMed](#)]
64. McNeill, H.; Reginensi, A. Lats1/2 Regulate Yap/Taz to Control Nephron Progenitor Epithelialization and Inhibit Myofibroblast Formation. *J. Am. Soc. Nephrol.* **2017**, *28*, 852–861. [[CrossRef](#)] [[PubMed](#)]
65. Shima, Y.; Miyabayashi, K.; Sato, T.; Suyama, M.; Ohkawa, Y.; Doi, M.; Okamura, H.; Suzuki, K. Fetal Leydig cells dedifferentiate and serve as adult Leydig stem cells. *Development* **2018**, *145*, dev169136. [[CrossRef](#)] [[PubMed](#)]
66. Liu, F.; Lagares, D.; Choi, K.M.; Stopfer, L.; Marinković, A.; Vrbanc, V.; Probst, C.K.; Hiemer, S.E.; Sisson, T.H.; Horowitz, J.C.; et al. Mechanosignaling through YAP and TAZ drives fibroblast activation and fibrosis. *Am. J. Physiol. Lung Cell. Mol. Physiol.* **2015**, *308*, L344–L357. [[CrossRef](#)]
67. Byun, J.; Del Re, D.P.; Zhai, P.; Ikeda, S.; Shirakabe, A.; Mizushima, W.; Miyamoto, S.; Brown, J.H.; Sadoshima, J. Yes-associated protein (YAP) mediates adaptive cardiac hypertrophy in response to pressure overload. *J. Biol. Chem.* **2019**, *294*, 3603–3617. [[CrossRef](#)]
68. Rinschen, M.M.; Grahammer, F.; Hoppe, A.-K.; Kohli, P.; Hagmann, H.; Kretz, O.; Bertsch, S.; Höhne, M.; Göbel, H.; Bartram, M.P.; et al. YAP-mediated mechanotransduction determines the podocyte's response to damage. *Sci. Signal.* **2017**, *10*, eaaf8165. [[CrossRef](#)]
69. St-Jean, G.; Tsoi, M.; Abedini, A.; Levasseur, A.; Rico, C.; Morin, M.; Djordjevic, B.; Miinalainen, I.; Kaarteenaho, R.; Paquet, M.; et al. Lats1 and Lats2 are required for the maintenance of multipotency in the Mullerian duct mesenchyme. *Development* **2019**, *146*, dev180430. [[CrossRef](#)]
70. Sonnylal, S.; Shi-Wen, X.; Leoni, P.; Naff, K.; Van Pelt, C.S.; Nakamura, H.; Leask, A.; Abraham, D.; Bou-Gharios, G.; de Crombrughe, B. Selective expression of connective tissue growth factor in fibroblasts in vivo promotes systemic tissue fibrosis. *Arthritis Rheum.* **2010**, *62*, 1523–1532. [[CrossRef](#)]
71. Lipson, K.E.; Wong, C.; Teng, Y.; Spong, S. CTGF is a central mediator of tissue remodeling and fibrosis and its inhibition can reverse the process of fibrosis. *Fibrogenesis Tissue Repair* **2012**, *5*, S24. [[CrossRef](#)] [[PubMed](#)]
72. Sakai, N.; Nakamura, M.; Lipson, K.E.; Miyake, T.; Kamikawa, Y.; Sagara, A.; Shinozaki, Y.; Kitajima, S.; Toyama, T.; Hara, A.; et al. Inhibition of CTGF ameliorates peritoneal fibrosis through suppression of fibroblast and myofibroblast accumulation and angiogenesis. *Sci. Rep.* **2017**, *7*, 5392. [[CrossRef](#)] [[PubMed](#)]
73. Yang, Z.; Sun, Z.; Liu, H.; Ren, Y.; Shao, D.; Zhang, W.; Lin, J.; Wolfram, J.; Wang, F.; Nie, S. Connective tissue growth factor stimulates the proliferation, migration and differentiation of lung fibroblasts during paraquat-induced pulmonary fibrosis. *Mol. Med. Rep.* **2015**, *12*, 1091–1097. [[CrossRef](#)] [[PubMed](#)]
74. Sonnylal, S.; Xu, S.; Jones, H.; Tam, A.; Sreeram, V.R.; Ponticos, M.; Norman, J.; Agrawal, P.; Abraham, D.; de Crombrughe, B. Connective tissue growth factor causes EMT-like cell fate changes in vivo and in vitro. *J. Cell Sci.* **2013**, *126*, 2164–2175. [[CrossRef](#)] [[PubMed](#)]
75. Garrett, Q.; Khaw, P.T.; Blalock, T.D.; Schultz, G.S.; Grotendorst, G.R.; Daniels, J.T. Involvement of CTGF in TGF-beta1-stimulation of myofibroblast differentiation and collagen matrix contraction in the presence of mechanical stress. *Investig. Ophthalmol. Vis. Sci.* **2004**, *45*, 1109–1116. [[CrossRef](#)] [[PubMed](#)]
76. Grotendorst, G.R.; Rahmanie, H.; Duncan, M.R. Combinatorial signaling pathways determine fibroblast proliferation and myofibroblast differentiation. *FASEB J.* **2004**, *18*, 469–479. [[CrossRef](#)]
77. Archambeault, D.R.; Yao, H.H. Activin A, a product of fetal Leydig cells, is a unique paracrine regulator of Sertoli cell proliferation and fetal testis cord expansion. *Proc. Natl. Acad. Sci. USA* **2010**, *107*, 10526–10531. [[CrossRef](#)]
78. Taylor, C.; Loomans, H.A.; Le Bras, G.F.; Koumangoye, R.B.; Romero-Morales, A.I.; Quast, L.L.; Zaika, A.I.; El-Rifai, W.; Andl, T.; Andl, C.D. Activin a signaling regulates cell invasion and proliferation in esophageal adenocarcinoma. *Oncotarget* **2015**, *6*, 34228–34244. [[CrossRef](#)]
79. Torigata, K.; Daisuke, O.; Mukai, S.; Hatanaka, A.; Ohka, F.; Motooka, D.; Nakamura, S.; Ohkawa, Y.; Yabuta, N.; Kondo, Y.; et al. LATS2 Positively Regulates Polycomb Repressive Complex 2. *PLoS ONE* **2016**, *11*, e0158562. [[CrossRef](#)]
80. Britschgi, A.; Duss, S.; Kim, S.; Couto, J.P.; Brinkhaus, H.; Koren, S.; De Silva, D.; Mertz, K.D.; Kaup, D.; Varga, Z.; et al. The Hippo kinases LATS1 and 2 control human breast cell fate via crosstalk with ER α . *Nature* **2017**, *541*, 541–545. [[CrossRef](#)]
81. Heallen, T.; Zhang, M.; Wang, J.; Bonilla-Claudio, M.; Klysik, E.; Johnson, R.L.; Martin, J.F. Hippo pathway inhibits Wnt signaling to restrain cardiomyocyte proliferation and heart size. *Science* **2011**, *332*, 458–461. [[CrossRef](#)] [[PubMed](#)]